Journal of Engineering Science and Technology Review 16 (3) (2023) 191 - 198

Research Article

JOURNAL OF
Engineering Science and Technology Review

www.jestr.org

3D Trajectory Planning of Agricultural Unmanned Aerial Vehicles Based on GA–SA Algorithm

Yusen Peng, Long Wang and Qixian Li *

School of Economics, Wuhan University of Technology, Wuhan 430000, China

Received 19 March 2023; Accepted 23 June 2023

Abstract

The trajectory optimization problem in agricultural unmanned aerial vehicles (UAVs) inspection of agricultural facilities and equipment shares similarities with the traveling salesman problem. Traditional heuristic algorithms can encounter challenges such as overlapping flight paths and local optima due to complex terrain, numerous obstacles, and external environmental influences. To optimize the agricultural UAV detection process, a Genetic Algorithm and Simulated Annealing (GA–SA) algorithm based on GA was proposed to calculate 3D flight paths for agricultural UAVs. By establishing a mathematical model that combines the UAV threat environment with physical constraints, the cost function of the traditional SA algorithm was optimized to improve search efficiency. Additionally, trajectory smoothing techniques were applied to ensure smooth transitions between trajectory points. Experimental results demonstrate that the GA–SA algorithm overcomes the limitations of the traditional SA algorithm in node search efficiency and trajectory smoothing, enabling the planning of realistic and optimal flight paths in 3D environments. The GA–SA algorithm exhibits an 18.82% improvement in convergence time GA–SA compared with the traditional GA algorithm and a 13.20% improvement compared with the SA algorithm. Moreover, it shortens the optimal track distance by 2.244 km and 1.793 km, respectively, validating the effectiveness of the proposed method.

Keywords: GA–SA algorithm, Agricultural unmanned aerial vehicles, 3D trajectory, Planning

1. Introduction

Agricultural unmanned aerial vehicles (UAVs) have emerged as modern agricultural machinery with various applications such as land and soil analysis, aerial seeding, spraying operations, crop monitoring, agricultural irrigation, and crop health assessment. As governments worldwide relax UAVs control regulations, enterprises have increasingly invested in agricultural UAV research and development, highlighting their significance in future agricultural production. Unmanned agriculture, an encompassing agricultural production process controlled through unmanned vehicles, agricultural UAVs, and satellite positioning systems, achieves true agricultural automation and modernization. By relying on transmitted UAV images and data, people can focus on judging and processing, thus optimizing agricultural operations. With the rapid development of artificial intelligence and machine learning technology, UAVs are finding their place in the agricultural field. Thanks to their high speed, efficiency, and precision, agricultural UAVs have become a popular technology in modern agriculture. However, the application value of agricultural UAVs cannot be fully realized without well-controlled trajectory planning. Thus, flight path planning for agricultural UAVs plays a crucial role.

When planning flight path routes, several factors must be considered. First, the altitude and speed of UAVs directly affect the effectiveness of agricultural operations. Improper altitude or speed may cause damage to farmland or result in unnecessary losses. Weather conditions also necessitate adjustments in UAVs' altitude and speed to ensure flight stability under conditions such as strong winds [1]. Additionally, terrain, vegetation, lighting, and other factors must be taken into account during planning. Achieving millimeter-level control over trajectory details is an inevitable trend to meet the accuracy requirements of UAVs' trajectory planning [2]. Trajectory planning for agricultural UAVs represents a fundamental technology that maximizes agricultural efficiency, reduces pesticide use and environmental pollution, promotes green agriculture, and enhances the agricultural industry.

Monitoring and controlling crop diseases and pests in the main stages of agricultural production heavily rely on manual labor, making the shortage of human resources increasingly evident. With the advancement of aerial application technology, agricultural UAVs have become widely used in modern agricultural production management. Utilizing UAVs for accurate monitoring, fertilization, and pesticide application has become an inevitable choice [3]. UAVs route planning is currently a research hotspot due to challenges such as poor manual operability and high operating costs [4]. The success or failure of flight missions directly depends on the reasonability of the trajectory planning for agricultural UAVs. In complex terrain environments like mountain orchards and farmlands, UAVs often encounter different types of threats and obstacles, including windshear areas, facilities, base station towers, forest protection trees, and agricultural buildings [5]. Therefore, reasonable and safe flight path planning for agricultural UAVs is essential to enhance their obstacle avoidance performance and reduce flight costs.

*E-mail address: m00klee@whut.edu.cn
ISSN: 1791-2377
doi:10.25103/jestr.163.23

2. State of the Art

In recent years, the increased use of UAVs in various fields, including military, industrial, and daily life, has driven the demand for autonomous flight capabilities. Path planning has been a major focus for scholars in related technical fields worldwide.

The UAVs' trajectory planning problem revolves around finding a safe and unobstructed path from the starting point to the target point in a 3D environment based on prior knowledge and mission requirements [6]. Currently, 3D path planning algorithms fall into two categories: traditional algorithms and intelligent algorithms. Traditional algorithms encompass methods such as the Rapidly-exploring Random Tree (RRT) algorithm [7], artificial potential field method [8], and A-star algorithm [9]. Intelligent algorithms include genetic algorithm [10], ant colony optimization algorithm [11], neural network algorithm [12], and particle swarm optimization algorithm [13]. To address limitations such as low efficiency and long, unsmooth paths in 3D path planning using the RRT algorithm, researchers have introduced heuristic functions oriented towards the target point and dynamic expansion step sizes [14]. Similarly, a mathematical model incorporating physical constraints of UAVs and environmental threat constraints has been proposed, resulting in an improved A-star algorithm based on model constraints [15]. Genetic algorithms (GA) have been enhanced by introducing the differential evolution mutation strategy and combining it with the simulated annealing (SA) algorithm to improve diversity and avoid local optima during mutation [16]. Combining ant colony optimization algorithms with artificial potential field methods, researchers have proposed a new pheromone updating mechanism and improved the heuristic function, significantly enhancing the algorithm convergence rate [17]. Traditional algorithms for path planning coupled with reinforcement learning have greatly improved UAVs' dynamic obstacle avoidance capabilities [18]. Intelligent algorithms, particularly those based on reinforcement learning and deep learning, have consistently performed well in the presence of dynamic obstacles, effectively identifying safe paths. Notably, the SA algorithm stands out due to its independence from extensive training data and lengthy training time while avoiding potential bias from training data in path generation. However, traditional SA algorithms often encounter challenges in terms of search efficiency and path complexity, presenting a path optimization dilemma. Researchers have reduced path generation complexity by decomposing the global map environment into multiple local environments, optimizing sub-node selection methods, improving cost functions, and introducing smoothing functions [19]. By incorporating a step-by-step search of key nodes, the directed SA algorithm has been enhanced, improving path-planning performance for mobile robots. However, these methods are primarily applied in two-dimensional environments [20]. In the case of 3D environments, the Kalman filtering algorithm is used to predict target positions, followed by path planning. Although flight range has been effectively reduced, path complexity remains high [21]. Under directional constraints, the SA algorithm generates numerous useless nodes. These methods have somewhat improved search efficiency and path planning for traditional SA algorithms, but challenges persist in 3D environments.

Heuristic algorithms, such as particle swarm optimization, GA, and SA algorithms, have been widely employed in route optimization research worldwide. For instance, an improved particle swarm optimization algorithm for multi-UAV cooperative route planning linearizes learning factors and proposes a speed adjustment mechanism, improving algorithm convergence rate. However, the particle swarm optimization algorithm may struggle with complex sample data, leading to locally optimal solutions [22]. Researchers have improved genetic algorithms by incorporating multiple constraints, utilizing the Surrounding Point Set (SPS) algorithm to generate initial populations faster, and employing the small environment method to maintain population diversity and avoid premature convergence [23]. Dynamic genetic algorithms have been utilized for unmanned aerial vehicle trajectory planning, optimizing crossover and mutation operators, and automatically adjusting probabilities based on individual fitness, resulting in advantages in optimization speed [24]. Although a single genetic algorithm can effectively solve optimal trajectories, as problem size increases, challenges such as difficulty in escaping local optima and low computational accuracy may arise during the optimization process. SA algorithms, which can accept different solutions based on the Metropolis criteria and possess strong local optimization capabilities, are widely used in trajectory optimization problems.

To improve the efficiency of SA algorithms in generating feasible neighborhood solutions, an exchange judgment strategy has been introduced in the optimization process, and virtual nodes have been added to the track optimization model, facilitating the acquisition of optimal solutions. Compared with traditional SA algorithms, the proposed method achieves shorter optimal track distances. However, SA algorithms often struggle with global optimization performance, potentially missing out on optimal global solutions if the cooling process is too fast [25]. Traditional SA algorithms exhibit certain drawbacks, including high computational load during planning stages and low algorithmic efficiency, resulting in obtained paths longer than the actual paths to target points, characterized by an excess of redundant nodes. To explore these issues, this study investigates the global optimization capability of the genetic algorithm and the local optimization capability of simulated annealing, GA–SA introducing a hybrid GA–SA algorithm to improve track optimization efficiency and reduce track distances. Taking the trajectory planning of agricultural UAVs as an example and considering the influence of complex spatial environments on the UAVs' trajectory, the proposed method's effectiveness is demonstrated through a comparative analysis of optimized UAVs trajectories using GA, SA and the hybrid GA–SA algorithm.

3. Model Construction

To explore the 3D trajectory planning problem for UAVs in a designated spatial area, a mathematical model needs to be established. This model should consider both the physical constraints of the UAVs and the complex impact of the environment on task execution, including special terrain conditions and radar detection threats.

3.1 Physical constraints of UAVs

Considering the physical constraints and task execution requirements of UAVs, the 3D trajectory planning should adhere to certain basic constraints, including:

(1) The minimum track segment length means that the UAV must maintain a direct flight distance before changing attitude. Assuming that the flight path of a UAV consists of and the minimum track segment length is L_{min} , the following conditions should be met:

$$L_i \geq L_{min} \tag{1}$$

(2) The maximum track segment length refers to the constraint that the flight track length of the UAV needs to be less than or equal to the preset maximum distance value. Assuming that the flight path of a UAV consists of $\{L| \quad i=1,2,3,\cdots,n\}$ and the maximum track segment length is L_{max}, the following conditions should be met:

In the weight of the topic keywords to be crawled by the web crawler, *TF·IDF* refers to the frequency of the web crawler crawling the behavior data of the power user group, and its calculation formula is as follows:

$$\sum_i \|L_i\| \leq L_{max} \tag{2}$$

In equation (2), $\|L_i\|$ represents the length of vector L_i.

(3) Maximum yaw angle pertains to the UAV turning within the maximum yaw angle range. Assuming the coordinate position of the track point is (x_i, y_i, z_i), the path vector of this segment is $s_i=(x_i-x_{i-1}, y_i-y_{i-1}, z_i-z_{i-1})$, and the maximum allowable yaw angle is φ_{max}. The following conditions should be met:

$$\frac{s_i^T s_{i+1}}{|s_i||s_{i+1}|} \geq \cos\varphi_{max} \tag{3}$$

In equation (3), s_i^T represents the transposition of the path vector and s_{i+1} represents the path vector of the next leg.

(4) The maximum climbing angle means the UAV is climbing within a certain height distance range. Assuming the maximum allowable climb angle is $\theta_{\max}$, the following conditions should be met:

$$\frac{|z_i - z_{i-1}|}{|s_i|} \leq \tan\theta_{\max} \tag{4}$$

In equation (4), $z_i - z_{i-1}|$ represents the absolute value of the climb altitude from $i-1$ to i and s_i represents the path vector of the segment.

(5) The minimum and maximum flight altitudes pertain to the UAV flying within a designated flight altitude range. Assuming that the flight altitude of the i th trajectory is H_i, the lowest flight altitude is $H_{\min}$, and the highest flight altitude is $H_{\max}$, the following conditions should be met:

$$H_{min} \leq H_i \leq H_{max} \tag{5}$$

(6) The maximum and minimum flight speeds refer to the constraint that the flight speed of a UAV on a certain flight path segment must be maintained within a limited range. Assuming that the flight speed of the UAV is V, the minimum flight speed is $V_{\min}$, and the maximum flight speed is $V_{\max}$, the following conditions should be met:

$$V_{min} \leq V \leq V_{max} \tag{6}$$

3.2 Threat environment model

Generally speaking, assuming that the central coordinate of a mountain in the planning area is (x_i, y_i, z_i), x, y represents longitude and latitude, z represents altitude, and a set of planning areas is

$$\{(x_i, y_i, z_i)| 0 \leq x_i \leq x_{\max}, 0 \leq y_i \leq y_{\max}, 0 \leq z_i \leq z_{\max}\} \tag{7}$$

In equation (7), $x_i \in (0, x_{\max})$ represents the range of longitude values, $y_i \in (0, y_{\max})$ represents the range of latitude values, and $z_i \in (0, z_{\max})$ represents the range of altitude values.

(1) Mountain threat model

In actual mission flight environments, UAVs need to use terrain to conceal their bodies. However, owing to the limitation of maximum flight altitude, they are prone to collide with mountains, leading to the destruction of UAVs [16]. In this study, the mountain is defined by an exponential function, and its mathematical model is

$$z_{Momtain}(x,y) = h(i)\sum_{i=1}^{n} \exp\left[-\left(\frac{x-x_i}{x_{si}}\right)^2 - \left(\frac{y-y_i}{y_{si}}\right)^2\right] \tag{8}$$

In equation (8), $z_{Momtain}(x,y)$ represents the elevation value at this point in the map; (x,y) represents the coordinates of the mountain center at that point; (x_i, y_i) represents the coordinates of the ith mountain center; x_{si} and y_{si} represent the reduction rates of the ith mountain along the x-axis and y-axis directions, respectively; and $h(i)$ represents terrain parameters.

(2) Radar threat model

Enemy detection radar is one of the biggest threats to UAVs during mission execution. The closer the body is to the radar, the higher the probability of detection and the greater the threat it poses to UAVs [17]. This study defines the radar detection range using a function expression, and its mathematical model is

$$z_{\text{Radsr}}(x,y) = K_{\text{h}}\left[R_{\max}^2 - (x-x_i)^2 - (y-y_i)^2\right] \tag{9}$$

In equation (9), $z_{\text{Radsr}}(x,y)$ represents the elevation value of the radar detection range, (x,y) represents the coordinates of the radar center at that location, (x_i, y_i) represents the coordinates of the ith radar center, K_{h} represents the value of radar detection performance coefficient, and $R_{\max}$ represents the maximum detection range value of the radar.

3.3 Mathematical model expression

The trajectory planning objective function of the UAV performing the task in this study is a collision-free flight path composed of a starting point and a target point. Assume that $Q_S(x,y,z,\varphi,\theta)$ represents the flight position and body attitude of the UAV, where (x,y,z) represents the UAV's coordinate position, φ represents the UAV's body turning angle, and θ represents the UAV's upward climb angle.

The objective function can be expressed as

$$Q_S(x_1,y_1,z_1,\varphi_1,\theta_1)\xrightarrow{r(Q)}Q_\Gamma(x_n,y_n,z_n,\varphi_n,\theta_n) \tag{10}$$

In the equation, Q_S and Q_Γ represent the starting point and target point, respectively; and $r(Q)$ represents a flight path from Q_S to Q_Γ.

Physical constraints can be expressed as

$$L_i \geq L_{max} \tag{11}$$

$$\varphi_i \leq \varphi_{max} \tag{12}$$

$$\theta_i \leq \theta_{max} \tag{13}$$

$$V_{min} \leq V_i \leq V_{max} \tag{14}$$

$$H_{min} \leq H_i \leq H_{max} \tag{15}$$

$$\sum_i \|L_i\| \leq L_{max} \tag{16}$$

Traditional SA algorithms typically search for nodes in eight sub-directions from the current node and use heuristic function values to determine the next extension node. However, when multiple minimum values exist, the algorithm cannot guarantee the optimal solution, leading to increased time costs. To address this issue, this study proposes the introduction of the GA and constructs the GA–SA algorithm. This algorithm transforms the search space of the traditional SA algorithm into a spatial region that satisfies the constraint function of the mathematical model, conducting node searches within this region. This method reduces the spatial range of the algorithm's search nodes and improves the search execution efficiency of the GA–SA algorithm.

4. Algorithm Design

In the problem of 3D path optimization for UAVs, as the scale of the problem increases, precise algorithms like linear programming become less applicable, and heuristic algorithms are widely employed.

4.1 Genetic algorithm

The GA algorithm is a random optimization search method that draws inspiration from the evolutionary principles of the biological world. It demonstrates the robustness and global search ability [15]. The GA algorithm begins with a randomly generated initial population and enhances population diversity through operations such as selection, crossover, and mutation. In this process, individuals are screened and eliminated based on their fitness. Individuals with good fitness undergo mating to generate a new population, and the iteration continues until the optimal individual is obtained. In the context of 3D trajectory optimization for UAVs, each individual in the GA algorithm corresponds to a UAV trajectory.

4.2 Simulated annealing algorithm

The SA algorithm is a heuristic random search algorithm based on the thermodynamic process of high-temperature solid cooling. The optimization process resembles the heating, isothermal, and cooling processes of solid annealing [16]. The SA algorithm starts with randomly generated or specific initial solutions and employs the random perturbation method to generate new solutions. It compares the objective function value of the new solution with the current solution and accepts the new solution with a certain probability according to the Metropolis criterion. This allows the algorithm to escape local optima and improve global convergence. The iteration continues until the end temperature is reached, and the optimal solution is output as the UAV's optimal trajectory. In the context of 3D trajectory optimization for UAVs, each solution in SA corresponds to a UAV trajectory.

4.3 Hybrid genetic simulated annealing algorithm

GA algorithm and SA algorithm are random optimization search methods. The GA algorithm exhibits robustness and strong global optimization ability but performs poorly in local optimization. In the later stages of the optimization search, the population's individuals tend to have high similarity, making it challenging to generate new individuals through crossover and variation, thereby hindering the ability to escape local optima [17]. SA can accept poor solutions with a certain probability and break out of local optima to find global optimal solutions. However, SA's global optimization ability is limited, and it is computationally inefficient.

Considering the advantages and disadvantages of the above two algorithms, a hybrid GA–SA algorithm is proposed to optimize the 3D trajectory of a UAV for transmission tower detection. To address the difficulty of generating new individuals through crossover and mutation in the later stages of the genetic algorithm search, crss mutation is applied to the genetic algorithm population, followed by simulated annealing to generate a new child population. This approach improves population diversity, enabling the genetic algorithm to escape local optima and obtain the optimal global solution. The GA–SA hybrid algorithm is used to solve the problem of 3D trajectory optimization for UAVs, and the calculation process is as follows:

Step 1: Code and generate the initial population. Encoding involves representing the chromosomes of individuals in the population using the integer arrangement encoding method. For the problem of optimizing the trajectory of agricultural UAVs performing n high-altitude safe hover views, the chromosome is divided into n segments, with each segment corresponding to a hover point sequence number. For example, in a track optimization problem involving five high-altitude {1, 2, 3, 4, 5} safe-hover agricultural UAVs, the chromosome |1|5|4|2|3| represents a valid solution. After completing the chromosome coding, an initial population is randomly generated, with the number of individuals determined by the size of the agricultural UAV's hover view.

Step 2: Calculate the fitness value for each individual. The fitness value serves as an index to evaluate the quality of chromosomes. The individual fitness evaluation function determines whether the maximum number of iterations has been reached. If the maximum number of iterations is reached, the optimal flight path for the agricultural UAV is output. Otherwise, proceed to Step 3.

Step 3: Perform the selection operation. The purpose of selection is to screen out individuals with higher fitness values and improve optimization efficiency. In this study, the roulette selection method is adopted, and the probability of individual i being selected in the iterative process is $P_i = \frac{E_i}{\sum_{i=1}^{N} E_i}$, where E_i is the individual fitness value and N is the initial population number.

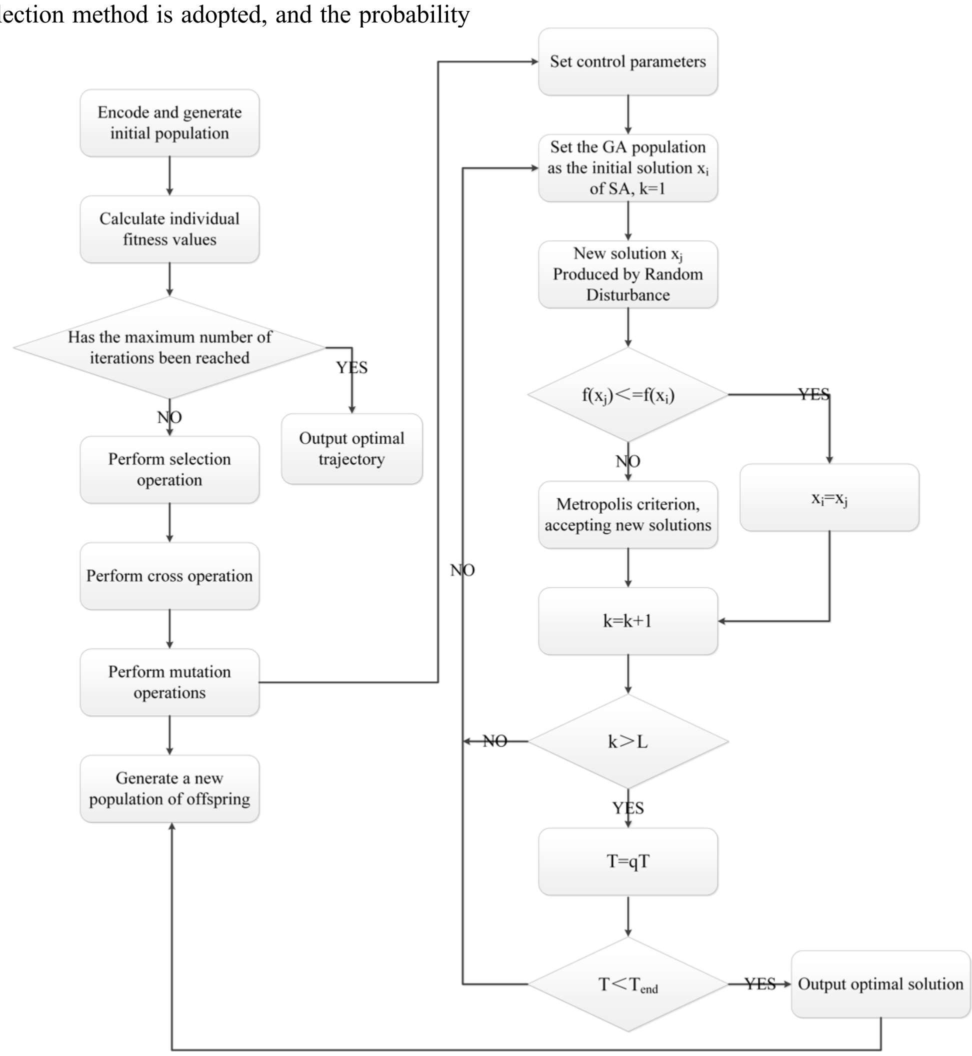

Fig.1. GA–SA operation flowchart

Step 4: Perform the crossover operation. The crossover operator is a key operator in the genetic algorithm, where two parents undergo crossover to produce a new individual. This study utilizes partial mapping hybridization, following these steps: (1) randomly select two sequence numbers representing high-altitude safety hover points of UAVs. Determine the positions of the two crossover points and exchange the data between them. (2) After crossover, if the same hover number exists in an individual, the local mapping method is used to eliminate duplicate hover numbers while retaining non-duplicate hover numbers.

Step 5: Perform the mutation operation. The mutation operator serves as an auxiliary operator, primarily providing the genetic algorithm with the ability for local random search. This study adopts the single-point mutation, where two sequence numbers representing UAV high-altitude safety hover views are randomly selected, their positions are exchanged, and a new individual is generated.

Step 6: Set the control parameters for the simulated annealing operation. To improve population diversity, the GA population undergoes the cross-mutation operation, followed by the simulated annealing operation. The control parameters for SA mainly include the initial temperature (T_0), end temperature (T_{end}), Metropolis chain length (L), and temperature attenuation factor (q).

Step 7: Set the crossed and mutated GA population individual as x_i, the initial solution of SA, and conduct simulated annealing operation on the GA population.

Step 8: Random perturbations generate new solutions x_j. The initial solution x_i is operated and a new UAV track is generated. The method of generating a new solution by random perturbation is to randomly select two hovering points from the current solution and exchange their positions to generate a new trajectory.

Step 9: Determine the size of the objective function of the new solution x_j and the initial solution x_i. Calculate the sizes of $f(x_j)$ and $f(x_i)$. If $f(x_j) \leqslant f(x_i)$, the new solution replaces the initial solution, and the number of iterations is increased by 1. Otherwise, go to Step 11.

Step 10: Accept the new solution with a certain probability according to the Metropolis criterion. The probability of accepting a new solution in the Metropolis criterion is $P_M = \exp\left[-\frac{f(x_j)-f(x_i)}{T}\right]$.

Step 11: Determine whether the number of iterations is greater than the Metropolis chain length (L). If it exceeds the length, apply the temperature attenuation factor (q) to cool down. Otherwise, return to Step 8.

Step 12: Determine whether the end temperature is reached. If $T<T_{end}$, output the current solution, otherwise go to Step 8 for the next iteration.

Step 13: Create a new offspring population. Select, crossover, and mutate individuals from the initial population of the genetic algorithm, then perform simulated annealing to generate new populations with higher fitness values. The new population is returned to Step 2 for individual fitness evaluation, and the iteration concludes. Refer to Fig. 1 for the flowchart of the hybrid GA–SA algorithm.

5. Simulation Experiment

5.1 Experimental environment and parameter settings

The simulation was conducted on a Windows 10 operating system using MATLAB 2014b. The mission planning area had dimensions of 20 km × 20 km, and the simulation model included randomly generated mountains and radar threats with radii ranging from 0.3km to 0.5km. The same 3D experimental environment was used for simulation verification. The coordinates of the main navigation points along the agricultural UAV's flight path are listed in Table 1.

Table 1. Main navigation points of agricultural UAV flight path

Serial number	X(km)	Y(km)	Z(km)
1	2	1	0.3
2	3	1	0.4
3	4	2	0.5
4	5	3	0.6
5	6	4	0.7
6	7	5	0.8
7	6	6	0.8
8	7	7	0.8
9	8	8	0.8
10	9	9	0.8
11	10	10	0.8
12	11	11	0.8
13	12	12	0.8
14	13	13	0.8
15	14	14	0.8
16	15	15	0.8
17	16	16	0.8
18	17	17	0.7
19	17	18	0.6
20	18	19	0.5
21	19	19	0.4
22	18	19	0.3

5.2 Experimental results

For the experiment, the starting point coordinates of the planned trajectory were set as (4, 10, 0.1), and the target point coordinates were (18, 20, 0.3). The GA–SA algorithm was run for a maximum of 500 iterations. The initial population size of GA was set to 50, with a crossover probability of 0.8 and a mutation probability of 0.2. The SA operation had an initial temperature of 98 ℃, an end temperature of 8 ℃, a temperature attenuation coefficient of 0.995, and a Metropolis chain length (L) of 300. The UAV's take-off point was set as (4, 10, 0.1) and the landing point as (18, 20, 0.3). The results of the GA–SA algorithm optimizing the 3D track for UAV inspection are shown in Figure 2.

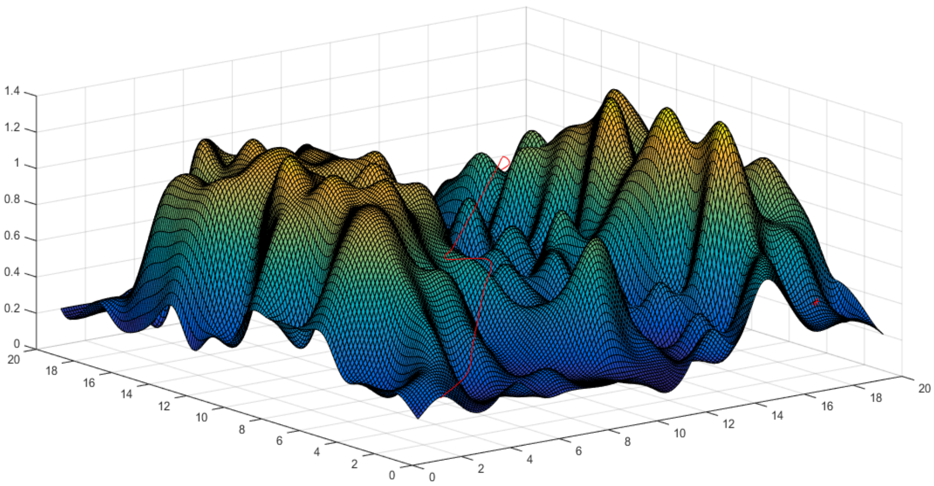

Fig. 2. GA–SA algorithm for agricultural UAV track planning

To visualize the 3D trajectory planning path of the agricultural UAV accurately, MATLAB 2014b was used to display the UAV's 3D flight path through a 3D coordinate system. The 3D flight path is shown in Figure 3.

To verify the effectiveness of the GA–SA algorithm, the GA, SA, and hybrid GA–SA algorithms were used to optimize the UAV's 3D track under the same environment, with a planned area of 20 km × 20 km and the same threat model position, starting point, and target coordinates. The comparison results of the convergence time and UAV track path length for the three algorithms are presented in Table 2.

Table 2. Comparison of results of the three algorithms

Algorithm	Algorithm Convergence Time (s)	Path Length (km)
GA algorithm	28.72	32.868
SA algorithm	27.36	32.417
GA-SA algorithm	24.17	30.624

As shown in Table 2, the convergence time of the GA–SA algorithm is 18.82% and 13.20% higher than that of the traditional GA and SA algorithm, respectively. Under the same experimental environment, the convergence time for the GA–SA algorithm was 4.55 seconds and 3.19 seconds, respectively. Additionally, the path length of the GA–SA algorithm is reduced by 7.33% and 5.85% compared with the traditional GA and SA algorithm, respectively. In the same experimental environment, the path length for the GA–SA algorithm was 2.244 km and 1.793 km, respectively. The simulation results demonstrate that the GA–SA algorithm not only improves the search speed of agricultural UAV trajectory planning but also reduces the path length of the trajectory planning. In terms of path search efficiency and algorithm optimization, the GA–SA algorithm outperforms the traditional GA and SA algorithm.

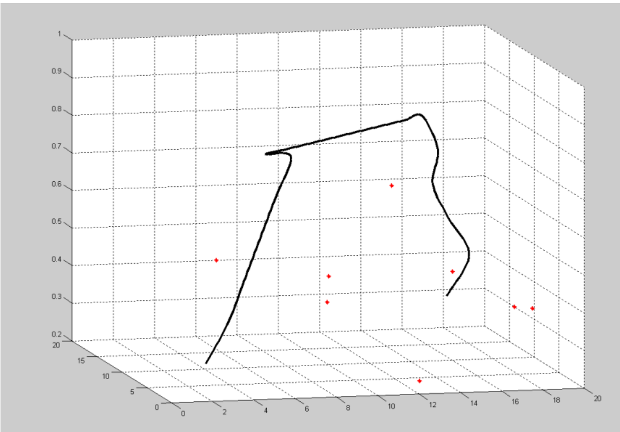

Fig. 3. 3D flight path of agricultural UAV in 3D coordinate system

Therefore, through the comparison of experimental results, the proposed GA–SA algorithm effectively avoids threats and plans the optimal flight path for UAV 3D trajectory planning. The algorithm successfully reduces the search time and shortens the path length of the trajectory planning, validating the effectiveness and progressiveness of the GA–SA algorithm proposed in this study.

6. Conclusion

In this study, a GA–SA hybrid algorithm for the trajectory planning of agricultural UAVs was proposed in the 3D environment. A mathematical model was established based on the physical constraints and threat environment of UAVs, defining the planned space region searched by the algorithm. The GA–SA algorithm incorporated weight GA–SA coefficients to guide the node search toward the target node, with different coefficient values set for different stages of the search path. Curve smoothing was employed to ensure smooth transitions between trajectory points and reduce sub-path lengths. This study conducted on the trajectory planning of agricultural UAVs led to the following conclusions:

(1) To improve the convergence speed and path distance of agricultural UAV 3D track planning, a GA–SA hybrid optimization algorithm was proposed, combining the genetic algorithm's strong global search ability with the genetic algorithm's fast local convergence speed.

(2) The GA–SA hybrid algorithm was successfully applied to plan the inspection trajectory of agricultural UAVs. Compared with the traditional GA and SA algorithm, the GA–SA algorithm showed an increased convergence time of 18.82% and 13.20%, respectively. The optimal track distance was reduced by 2.244 km and 1.793 km, respectively, validating the effectiveness of the proposed method. This study provides valuable insights for ensuring the flight path planning of agricultural UAVs and improving UAV's flight path planning efficiency.

References

1. Dong, J., Chu, H. S., Lu, Y. Z., Tang, L. L., Dai, J. L. "Research on UAV path planning optimization model based on A-star algorithm". *Hydrographic Surveying and Charting*, 41(3), 2021, pp. 28-31, 51.
2. Chen, H. Y., Chen, H. Z., Liu, Q. "Multi-UAV 3D formation path planning based on improved artificial potential field". *Journal of System Simulation*, 32(3), 2020, pp. 414-420.
3. Fan, Y. M., Chen, K. C., Wang, D., Zhai, C. Y., Zhang, H. H. "Optimal energy consumption path planning of UAV on mountain region based on simulated annealing algorithm". *Transactions of the Chinese Society for Agricultural Machinery*, 51(10), 2020, pp. 34-41.
4. Jiang, Y. J., Li, Z. Y., Guan, Q. X., Guan, S. J. "Research on UAV path planning based on improved A-star algorithms". *Journal of Ordnance Equipment Engineering*, 41(9), 2020, pp. 160-164.
5. Chen, X., Liu, K. W., Mao, H. L. "UAV path planning based on APF-RRT algorithm". *Electronics Optics & Control*, 29(5), 2022, pp. 17-22.
6. Ou, M. Y., Sun, H. B., Zhang, Z. X,, Gu, S. W. "Fixed-time trajectory tracking control for nonholonomic mobile robot based on visual servoing". *Nonlinear Dynamics*, 108(1), 2022, pp. 251-263.
7. Wang, F., Chao, Z. Q., Huang, L. B., Zhang, C. Q. "Trajectory tracking control of robot manipulator based on RBF neural network and fuzzy sliding mode". *Cluster Computing*, 16(7), 2017, pp. 1-11.
8. Kattenborn, T., Eichel, J., Fassnacht, E. F. "Convolutional neural networks enable efficient, accurate and fine-grained segmentation of plant species and communities from high-resolution UAV imagery". *Scientific Reports*, 9(1), 2019, pp. 17656.
9. Stanton, C. M., Kalonde, P., Zembere, K., Spaans, H. R., Jones, M. C. "The application of drones for mosquito larval habitat identification in rural environments: a practical approach for malaria control?". *Malaria Journal*, 20, 2021, pp. 244.
10. Wang, G., Zhou, J. "Dynamic robot path planning system using neural network". *Journal of Intelligent Fuzzy Systems*, 40(2), 2021, pp. 3055-3063.
11. Peng, H. J., Li, F., Liu, J. G., Ju, Z. J. "A Symplectic instantaneous optimal control for robot trajectory tracking with differential-algebraic equation models". *IEEE Transactions on Industrial Electronics*, 67(5), 2020, pp. 3819-3829.
12. Majd, K., Razeghi-Jahromi M., Homaifar, A. "A stable analytical solution method for car-like robot trajectory tracking and optimization". *IEEE/CAA Journal of Automatica Sinica*, 7(1), 2020, pp. 39-47.
13. Hodgson, C. J., Mott, R., Baylis, M. S., Pham, T. T., Wotherspoon, S., Kilpatrick, A. D., Raja Segaran, R., Reid, I., Terauds, A., Koh, L. P. "Drones count wildlife more accurately and precisely than humans". *Methods in Ecology and Evolution,* 9(5), 2018, pp. 1160-1167.
14. Qin, H., Shao, S., Wang, T., Yu, X., Jiang, Y., Cao, Z. "Review of autonomous path planning algorithms for mobile robots". *Drones*, 7(3), 2023, p. 211.
15. Peng, J., Xu, W. F., Yang, T. W., Hu, Z. H., Liang, B. "Dynamic modeling and trajectory tracking control method of segmented linkage cable-driven hyper-redundant robot". *Nonlinear Dynamics*, 101(1), 2020, pp. 233-253.
16. Randis, R. "Uji eksperimetal trajectory tracking pada robot penjinak bom". *Jurnal Integrasi*, 11(1), 2019, pp. 33-36.

17. Khalilpour, A. S., Khorrambakht, R., Damirchi, H., Taghirad, H. D., Cardou, P. “Tip-trajectory tracking control of a deployable cable-driven robot via output redefinition”. *Multibody System Dynamics*, 16(4), 2020, pp. 1-28.
18. Wu, C., Liu, Z., Zhang, D., Yoshinaga, T., Ji, Y. “Spatial intelligence toward trustworthy vehicular IoT”. *IEEE Communications Magazine*, 56(10), 2018, pp. 22-27.
19. Guo, T., Yu, K. P., Aloqaily, M., Wan, S. H. “Constructing a prior-dependent graph for data clustering and dimension reduction in the edge of AIoT”. *Future Generation Computer Systems*, 128, 2022, pp. 381-394.
20. Bensafia, Y., Ladaci, S., Khettab, K., Chemori, A. “Fractional order model reference adaptive control for SCARA robot trajectory tracking”. *International Journal of Industrial and Systems Engineering*, 30(2), 2018, pp. 138-156.
21. Oubbati, O. S., Chaib, N., Lakas, A., Lorenz, P., Rachedi, A. “UAV-assisted supporting services connectivity in urban VANETs”. *IEEE Transactions on Vehicular Technology*, 68(4), 2019, pp. 3944-3951.
22. Shahzad H., Qurratul-Ain M., Sheeraz A., Asif N. “Nature inspired optimization techniques, A review for FANETs”. *Electronics Optics & Control*, 3(2), 2020, pp. 40-58.
23. Eschmann, H., Ebel, H., Eberhard, P. “Trajectory tracking of an omnidirectional mobile robot using Gaussian process regression”. *Automatisierungstechnik*, 69(8), 2021, pp. 656-666.
24. Gan, C., Cao, W. H., Wu, M., Chen, X. “A new bat algorithm based on iterative local search and stochastic inertia weight”. *Expert Systems with Applications*, 104, 2018, pp. 202-212.
25. Lyu, S. L., Li, Z., Huang, Y. L., Hu, J. “Improved self-adaptive bat algorithm with step-control and mutation mechanisms”. *Journal of Computational Science*, 30, 2019, pp. 65-78.